

## Effects of mountain barrier on a barotropic jet\*

HAJIME NAKAMURA

Geophysical Institute, Tokyo University, Japan

**सारांश** — इस लेख में अत्यधिक प्रवण पर्वतीय अवरोध के वायु प्रवाह पर प्रभाव का अध्ययन किया गया है। अवरोध की तीव्रता पर्वत की प्रवणता तथा उसकी ऊंचाई पर निर्भर करती है। सपाट अथवा कम प्रवणता वाला पर्वत वायु के प्रवाह को नहीं रोकता है तथा अमिल नलिका का फैलने और सिकुड़ने वाला गुण स्थिर ग्रहीय तरंगें पैदा करता है जबकि एक प्रवण-पर्वत वायु प्रवाह को रोकता है तथा तरंगें नहीं उत्पन्न होती। पूर्वी एशिया में पछुआ जेट की रचना तथा उसकी गति पर पर्वतों के गतिकीय प्रभाव के लिये इसका अध्ययन किया गया है।

**ABSTRACT.** In the present paper effect of mountain barrier which is very steep on a airflow has been studied. The intensity of blocking effect depends on the steepness of a mountain as well as on the height. A smooth mountain does not block the flow and hence the stretching and shrinking effect of vortex tube produces stationary planetary waves, while a steep mountain blocks the flow and the waves are not produced. For this purpose westerly jet has been studied to see the dynamical effect of the mountains on its structure and movement over the eastern Asia.

### 1. BLOCKING EFFECT AND STRETCHING AND SHRINKING EFFECT OF VORTEX TUBE

#### 1. Introduction

One of the central problems about the dynamical effects of mountains on large-scale motions of the atmosphere is the production of stationary planetary waves by large-scale topography. The generally accepted explanation for the generation of stationary planetary waves is based on the conservation of the absolute potential vorticity. When a westerly flow climbs up a mountain slope a vortex tube on the flow shrinks and gains anticyclonic vorticity, while it stretches and becomes cyclonic when the westerly flow slides down the slope. Thus the vortex tube changes its position from the original latitude simultaneously. It must be restored to the original latitude by the  $\beta$ -effect so that the absolute potential vorticity is conserved and hence an oscillation occurs in the downstream of the mountain.

In the above explanation it is assumed implicitly that the westerly flow always crosses over a mountain. However, if a mountain is very steep, air flow cannot climb it and may be blocked by the mountain. In such a case the mechanism mentioned above does not work. Instead there may occur a flow which goes around the mountain. There is a possibility that this flow in turn makes a stationary trough in the leeside of the mountain.

The intensity of the blocking effect depends on the steepness of a mountain as well as on the height. It may be speculated that a smooth mountain does not

block the flow and hence the stretching and shrinking effect of vortex tube produces stationary planetary waves, while a steep mountain blocks the flow and the waves are not produced. It is interesting to investigate the possibility of this mechanism. It is also important as a problem of numerical modelling of the effects of mountains, because it is usual to incorporate smoothed mountains in the general circulation models and numerical prediction models in order to avoid the possibility that steep mountains may have large truncation errors.

#### 2. Model and mountains

We consider a westerly jet and study what flow pattern is established as a steady state (if it exists), when a mountain is placed in the jet. We assume for the sake of simplicity that the atmosphere has a stable stratification in the vertical but has no temperature gradient in the horizontal direction in the basic state. There is a force which acts to bring the flow to a barotropic equilibrium state which has a jet with a prescribed profile.

$$\frac{\partial u}{\partial t} + \dots = -\alpha(u - u_e), \quad \frac{\partial v}{\partial t} + \dots = -\alpha(v - v_e)$$

and

$$\frac{\partial T}{\partial t} + \dots = -\beta(T - T_e)$$

where  $u_e$ ,  $v_e$  and  $T_e$  are the  $u$  and  $v$ -components of the wind and temperature in the equilibrium state.  $\alpha$  and  $\beta$  are constants assigned to be 1/10 day.  $u_e$ ,  $v_e$  and  $T_e$  are assumed as

$$u_e(\phi) = u_0 \sin^2 2\phi \quad \text{and} \quad v_e = 0$$

where  $u_0 = 50$  m/s. and  $T_e$  is expressed by

$$T_e(\phi, z) = T_e^s(\phi) - \Gamma z$$

\*Paper was presented at the symposium on "Indo-French School on recent advances in Computer Techniques in Meteorology, Bio-mechanics and Applied Systems" held at I.I.T., New Delhi, 4-13 February 1980

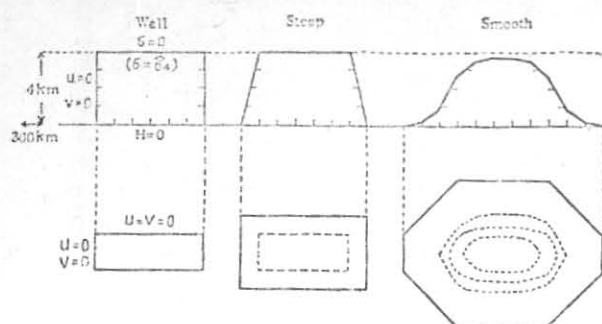


Fig. 1. Shapes of the smooth, steep and wall mountains



GEO-POTENTIAL HEIGHT (100M) ST=07.00  
 0 YR 10 DAY 0 HR 0 MIN 0 SEC 80.11.00

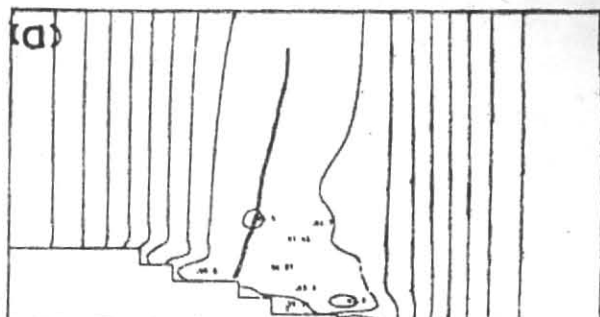


GEO-POTENTIAL HEIGHT (100M) ST=07.00  
 0 YR 10 DAY 0 HR 0 MIN 0 SEC 80.11.00

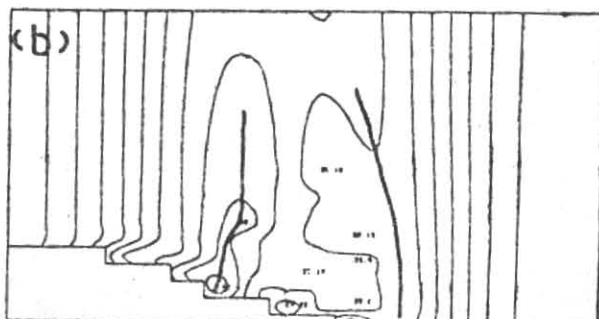


GEO-POTENTIAL HEIGHT (100M) ST=07.00  
 0 YR 10 DAY 0 HR 0 MIN 0 SEC 80.11.00

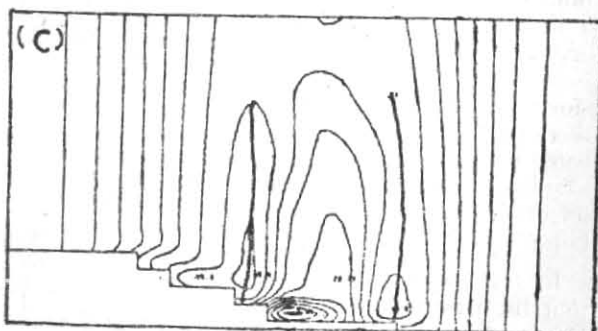
Fig. 2. Patterns of the geopotential height at 500 mb at day 10 for the (a) Smooth, (b) Steep and (c) Wall mountains. Dashed line and dotted line in the centre of the figures show the mountains



ZONAL WIND (M/SEC) ST=0.00  
 L-M ZONAL MEAN 0 YR 10 DAY 0 HR 0 MIN 0 SEC 80.5.00



ZONAL WIND (M/SEC) ST=0.00  
 L-M ZONAL MEAN 0 YR 10 DAY 0 HR 0 MIN 0 SEC 80.5.00



ZONAL WIND (M/SEC) ST=0.00  
 L-M ZONAL MEAN 0 YR 10 DAY 0 HR 0 MIN 0 SEC 80.5.00

Fig. 3. Latitude-height distribution of the zonal mean wind at day 10 for the (a) Smooth, (b) Steep and (c) Wall mountains. Contour width is 5 m/s. The left and right side of the figure are the pole and the equator, respectively. The top of the figure is at 100 mb and the bottom is 1,050 mb

where  $\Gamma$  is set to be  $6.5^\circ \text{ K/km}$ .

The model is a half-hemispheric 6 layers model with the horizontal grid size of  $5^\circ$  and the top of 100 mb.

The three types of idealized mountains shown in Fig. 1 are incorporated in the model. The height of the steep mountain is 4 km. The inclination of its side slopes is  $4 \text{ km}/5^\circ$ . The smooth mountain is obtained by operating a smoothing method used by Holloway and Manabe (1971). The other type is the wall mountain. We assume an impenetrative stagnant air mass as the mountain. This assumption is the same as that of Egger (1972).

### 3. Result

Fig. 2 shows the geopotential height at 500 mb at day 10. Over the smooth mountain the flow turns its direction southward strongly and a deep trough appears in the lee of the mountain. In the case of the steep mountain the jet is a little weaker than that of the smooth mountain and the trough in the lee of the mountain is not so deep. The pattern of the wall mountain is more zonal than those of the other mountains. The jet and the trough is the weakest.

Fig. 3 shows latitude-height distributions of the zonal mean winds. We see that in the case of the smooth mountain the blocking effect is very weak and the jet crosses over the mountain and there is only one maximum. On the contrary, the jet is blocked and goes around the mountain so that two maxima appear at the latitudes which correspond to the northern and southern boundaries of the mountain in the cases of the steep and wall mountains. The intensity of the jet is reduced more largely by the wall mountain than the steep mountain. This may be explained by the fact that the wall mountain has the vertical side boundaries while the steep mountain has the sloped side boundaries.

There is a difference in the formation of stationary planetary waves in the lee of the mountains. In Fig. 4 we see that the amplitude of the perturbed geopotential height in the downstream is the largest for the smooth mountain. It is about 400 m at 500 mb level. For the wall and steep mountains they are about 200 m and 300 m respectively. Moreover, positions of the troughs differ by about  $10^\circ$  between the smooth and steep mountains and also between the steep and wall mountains.

These results may be explained as follows: The steep and wall mountains block the westerly flow well so that there are weak flows over the mountains, while the smooth mountain blocks the flow weakly so that the flow over the mountain is stronger than those of the other two. Since the stretching and shrinking of vortex tube occurs in a flow which climbs up and down the mountain slopes, it is speculated that stretching and shrinking of vortex tube over the smooth mountain is greater than over the steep and wall mountains. Therefore, the stationary planetary trough in the downstream is strongest in the case of the smooth mountain.

## II. SPLITTING OF A JET

### 1. Introduction

Next a numerical simulation is made to explain the splitting of a jet by a mountain. Staff members of Academia Sinica (1957) studied the flow pattern over the eastern Asia. They showed that there are two maxima of the jet over the northern and southern boundaries of the Tibetan Plateau during the period from autumn to spring. From spring to summer, however, the southern branch of the jet disappears suddenly and there is a single jet in summer. This phenomenon was also noticed by Murakami (1951) in relation with the jet stream over the Asia in the Baiu season (rainy season in Japan). The appearance of the double or single jet may be explained as the result of the seasonal displacement of the jet axis.

### 2. Model and jets

We use the steep mountain which is regarded as the Tibetan Plateau.

For the present experiment, we need to change the position of the jet axis relative to the mountain. Therefore,  $u_e$  is changed as

$$u_e = \frac{u_0}{\cosh \{(\phi - \phi_0) / \delta\}}$$

where  $u_0$  is the maximum wind velocity at the jet axis  $\phi_0$  is the latitude of the jet axis and  $\delta$  is a parameter to specify the width of the jet. We test various values of  $u_0$ ,  $\phi_0$  and  $\delta$  and obtain three jets named as the J35, J45 and J55 shown in Fig. 5. The mountain is situated between  $34^\circ$  and  $55^\circ$  latitudes. The J35 passes by the southern boundary of the mountain and the J45 hits the mountain directly. The J55 passes by the northern boundary of the mountain. Relative positions of the three jet axes to the mountain correspond to the seasonal change of the position of the westerly jet in the real atmosphere. That is, J35 corresponds to the jet in winter, the J55 in summer and the J45 in spring and autumn.

### 3. Results

Fig. 6 shows flow patterns at 750 mb when the mountain is included. The main axis of the J35 shifts northward on the average compared with the case of no mountain. In the mountain region a considerably strong branch of a jet goes around the northern side of the mountain. The southern branch shifts southern by about  $10^\circ$  from the latitude of the main axis in the upstream of the mountain.

The main axis of the J45 is located at about  $47.5^\circ$  in the upstream of the mountain and passes by the northern side of the mountain but becomes weak in the lee side of the mountain. The southern branch of the jet becomes strong to the south of the mountain and the two jets confluent at about  $20^\circ$  downstream of the mountain. The trough in the downstream is stronger than that of the J35.

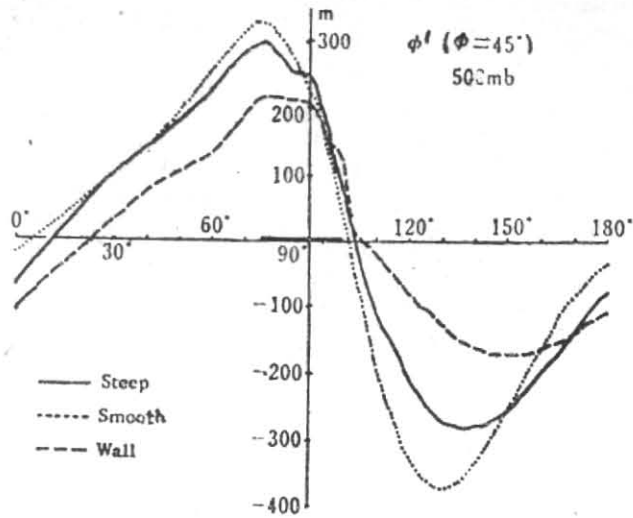
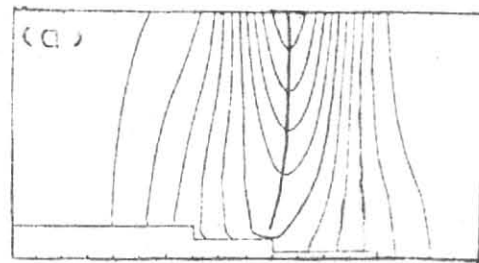
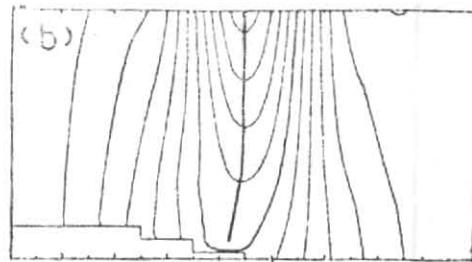


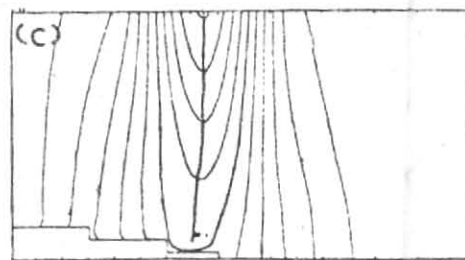
Fig. 4. Deviations of the geopotential height at 500 mb along 45° latitude for the smooth (dotted line), steep (solid line) and wall mountain (dashed line) at day 10.



ZONAL WIND (M/SEC) 210.00  
L-H ZONAL MEAN 0 TA 8 DAY 0 HR 0 MIN 0 SEC 045.00



ZONAL WIND (M/SEC) 510.00  
L-H ZONAL MEAN 0 TA 8 DAY 0 HR 0 MIN 0 SEC 045.00



ZONAL WIND (M/SEC) 140.00  
L-H ZONAL MEAN 0 TA 8 DAY 0 HR 0 MIN 0 SEC 045.00

Fig. 5. Latitude-height distributions of the zonal mean wind at day 8 with no mountain for the (a) J35, (b) J45, (c) J55

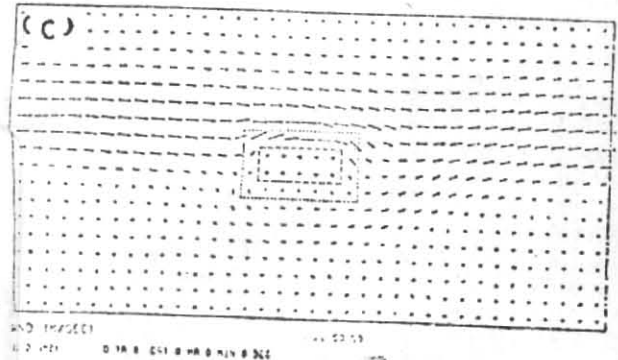
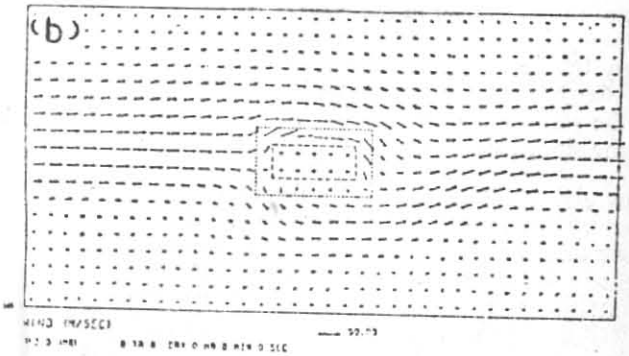
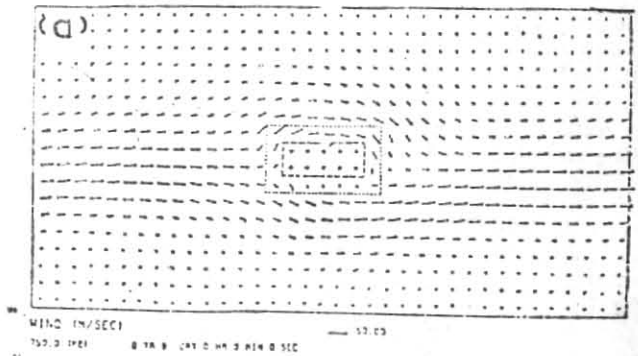
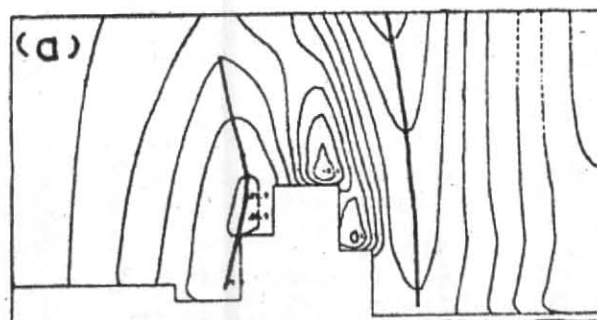
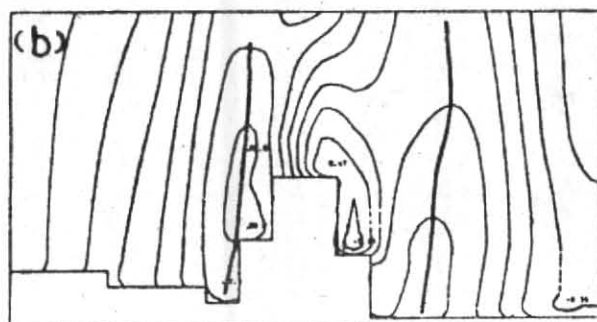


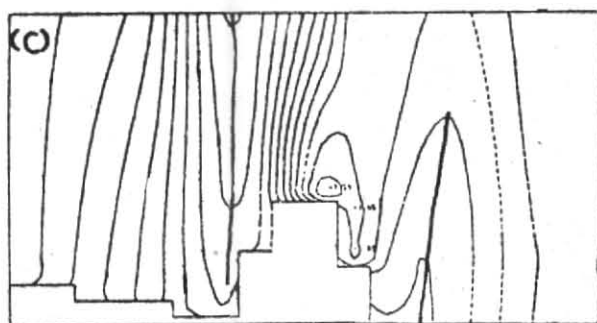
Fig. 6. Patterns of the wind vectors at 750 mb at day 8 with the mountain for: (a) J35, (b) J45 and (c) J55



ZONAL WIND (M/SEC) ST=0.00  
 L-H 87.50 (DEG) 0 YR 0 DAY 0 HR 0 MIN 0 SEC BD=5.00



ZONAL WIND (M/SEC) ST=0.00  
 L-H 87.50 (DEG) 0 YR 0 DAY 0 HR 0 MIN 0 SEC BD=5.00



ZONAL WIND (M/SEC) ST=0.00  
 L-H 87.50 (DEG) 0 YR 0 DAY 0 HR 0 MIN 0 SEC BD=5.00

Fig. 7. Latitude-height distribution of the  $u$ -component of the wind at  $87.5^\circ$  (latitude): (a) J35, (b) J45, (c) J55

The axis of the J55 is located at  $55^\circ$  and shifts only little by the mountain. The southern branch of the jet also appears but is very weak compared to those of the J35 and J45.

Fig. 7 shows the double jet structures in the mountain region. In the J35 the main axis is by about  $10^\circ$  southward from the mountain and the wind increases with height. Another branch appears over the northern slope of the mountain, which has its maximum just above the slope and becomes weak with increasing height and disappears in the upper atmosphere. In the J45 the main axis shifts to the northern slope of the mountain and the secondary branch appears at  $30^\circ$  latitude. This has an inverse vertical shear as same as the northern branch of the J35. Unlike the J35, the magnitude of the main jet decreases with height and its axis tilts southward. In the J55 the change of the pattern due to the mountain is smaller than those of the other jets. The main jet is located almost at the same latitude as that in the zonal mean field. There appears a southern branch but it is very weak compared with the secondary axes of the other jets.

The three jet patterns seem to explain the seasonal positions of the jet over the eastern Asia reported by staff members of Academia Sinica. The pattern of the J35 corresponds to the flow in winter when the jet shifts most southward to the southern side of the Tibetan

Plateau and the double maxima appear. The J45 shows the pattern in spring when the jet shifts gradually to the north and hits the plateau directly. In this case two maxima appear as well as in winter. The J55 shows the flow in summer when there is a single jet to the north of the plateau. However, since in the real atmosphere the westerly jet is maintained by baroclinicity which is neglected in this experiment, it will be necessary to consider the effect of baroclinicity in the accurate discussion of the dynamical effects of mountains.

#### References

- Egger, J., 1972, Incorporation of steep mountains into numerical forecasting models, *Tellus*, **24**, 325-335.
- Holloway, J.L. (Jr.) and Manabe, S., 1971, Simulation of climate by a global general circulation model. I. Hydrologic cycle and heat balance, *Mon. Weath. Rev.*, **99**, 335-370.
- Murakami, T., 1951, On the study of the change of the upper westerlies in the last stage of the Baiu season (Rainy season in Japan) (in Japanese), *J. met. Soc. Japan*, **29**, 162-175.
- Nakamura, H., 1978, Dynamical effects of mountains on the general circulation in the atmosphere, *J. met. Soc. Japan*, **56**, 317-367.
- Staff members of Academia Sinica, Peking, 1957, On the general circulation over Eastern Asia (I), *Tellus*, **9**, 433-446.